Atomic structure and SiH_4-H_2 interactions of $SiH_4(H_2)_2$ from first principles

Kyle Michel, Yongduo Liu, and Vidvuds Ozolins*
Department of Materials Science and Engineering, University of California–Los Angeles, P.O. Box 951595, Los Angeles, California 90095-1595, USA

(Received 1 November 2009; revised manuscript received 11 October 2010; published 3 November 2010)

First-principles density-functional theory (DFT) calculations are used to understand the crystal structure, bonding, and vibrational properties of the recently discovered high-pressure $SiH_4(H_2)_2$ compound. We find a general decrease in the frequencies of the intramolecular H_2 stretching modes with increasing pressure, where the tetrahedral H_2 exhibit markedly stronger softening than octahedral H_2. Our DFT results suggest a weakening of the H_2 bond that is explained by increased orbital overlap and electron sharing between the silane and hydrogen molecules, which also account for the unusually high hydrogen capacity of $SiH_4(H_2)_2$.

DOI: 10.1103/PhysRevB.82.174103 PACS number(s): 61.50.Ah

I. INTRODUCTION

Hydrogen-matter interactions are conventionally divided into two broad, nonoverlapping classes: physisorption and chemisorption. While physisorption does not disturb the intramolecular H_2 bond, chemisorption dissociates the H_2 molecules into individual hydrogen ions,[1] which subsequently form chemical bonds with the host. The discovery of the $SiH_4(H_2)_2$ compound[2,3] demonstrates that hydrogen-matter interactions can be considerably more complicated than those allowed by this conventional scheme. Bonding in this material exhibits an intermediate behavior where the H_2 molecular bond is largely preserved but where orbital overlap leads to electron sharing and chemical binding between H_2 and the host SiH_4. It also opens up the intriguing possibility that there may be materials with this mixed type of bonding under ambient conditions that could offer a long sought-after combination of fast hydrogen uptake kinetics with improved hydrogen binding enthalpies that would be compatible with the requirements for reversible storage in fuel cell vehicles.[4]

Based on their experimental x-ray results, Strobel *et al.* proposed a structure for the compound $SiH_4(H_2)_2$ that belongs to the $F\bar{4}3m$ space group. The conventional cell for this structure contains four formula units and has a lattice constant of $a=6.426$ Å at a pressure of 6.8 GPa. Experimental data shows that SiH_4 units are centered at the sites of a face-centered cubic (fcc) lattice.[2] While the location of H_2 could not be determined directly, it was suggested that they are found in all of the octahedral and half of the tetrahedral voids. Contrary to the behavior of bulk H_2 under pressure,[5] Raman measurements on $SiH_4(H_2)_2$ revealed a pressure-induced decrease in the intramolecular vibrational frequencies of H_2.

In this paper, we present a comprehensive first-principles study of the structural, vibrational, and bonding properties of $SiH_4(H_2)_2$ using density-functional theory (DFT) techniques. We find that the energetically preferred orientation of silane units points their hydrogen ions toward the unoccupied tetrahedral interstices. The energetically preferred orientation of H_2 molecules at $T=0$ K is along the [100] direction but orientational disorder sets in at room temperature due to small energy differences between different H_2 orientations. Analysis of the electronic structure reveals electron sharing between H_2 and SiH_4, with the effect being stronger for the tetrahedral hydrogen than for the octahedral hydrogen. Different pressure dependences of the measured Raman peaks is attributed to the two types of H_2. While the frequencies of octahedral H_2 stay approximately constant (or even slightly increase at the lowest pressures), those of tetrahedral H_2 decrease with increasing pressure due to enhanced orbital overlap and electron sharing with SiH_4.

II. METHODS

In order to determine the location of hydrogen atoms in $SiH_4(H_2)_2$, SiH_4, and H_2 orientations are systematically enumerated.[6] In this method, all symmetry-inequivalent unit cells and molecular orderings are generated for structures that contain up to a given maximum number of formula units. These structures are relaxed to their static equilibrium configurations using DFT calculations and the total energies of these candidate configurations are used to select the most favorable $T=0$ K crystal structure. DFT total-energy calculations are performed using the highly efficient VASP (Ref. 7) code. Projector augmented wave potentials[8] and the generalized gradient approximation of Perdew and Wang[9] are used in all total-energy calculations. The plane-wave cutoff energy is fixed to 875 eV with regular $8\times8\times8$ Monkhorst-Pack[10] **k**-point meshes in the Brillouin zone. With these settings we find that the electronic energy is converged to better than 0.01 meV/H_2 for a given structure when compared to calculations using a $12\times12\times12$ **k**-point mesh. As the goals of this study are to explain the results seen in experimental work, during relaxations we have chosen to fix the volume per conventional cell (four formula units) to the experimentally determined value[2] of $V=265.35$ Å^3 (corresponding to a calculated pressure of 5.6 GPa) while the cell shape and atomic positions are allowed to relax. Enumerations are only carried out at this volume while higher pressure structures are relaxed with reduced volumes from the lowest-energy structure that is found. Nudged elastic band calculations[11] are used in order to find rotational barriers of H_2.

III. RESULTS AND DISCUSSION

During enumeration of $SiH_4(H_2)_2$ structures, the orientations of H_2 and SiH_4 units are treated separately as the number of possible combinations is much too large to be evaluated effectively if the two types are accounted for simultaneously. SiH_4 unit orientations are enumerated first with all H_2 set to lie in the [100] direction; this is found to be a sufficiently accurate approximation as the effect of the orientation of H_2 on the total energy is many times less than that of SiH_4 orientations. SiH_4 units are initially oriented in one of four configurations; these are chosen such that H ions are positioned on twenty distinct sites around the Si ion. Following relaxation of the enumerated structures, those that are the lowest in energy have all four SiH_4 units oriented along the $[\bar{1}\bar{1}\bar{1}]$, $[11\bar{1}]$, $[1\bar{1}1]$, and $[\bar{1}11]$ directions where corner H ions pointing toward unoccupied tetrahedral sites.

When enumerating H_2 orientations, all pairs are set to lie along any of the {100}, {110}, or {111} families of directions while SiH_4 groups are in their lowest-energy configuration. Following relaxations, structures with all H_2 dimers pointing in the {100} directions are found to be the lowest in energy. Relative to the average energy of the {100} oriented pairs, those oriented in the {110} and {111} directions are on average higher in energy by 4.7 meV/H_2 and 7.5 meV/H_2, respectively. Various structures with mixed H_2 orientations were also considered but all are found to be higher in energy than those with all pairs oriented along the [100] direction. Finally, we position H_2 molecules on tetrahedral sites other than those occupied in the diamond cubic structure and find this is highly energetically unfavorable by more than 1 eV/H_2, supporting similar conclusions proposed in experimental work.[2] Volume differences between competing structures at a given pressure are small and will lead to enthalpy corrections of less than 1 meV/f.u.[12]

We have also investigated the effect of phonons on the energetics using the supercell force constant approach.[13] Vibrational free energies were obtained by summing over calculated frequencies in a 288-atom supercell. Although this produces a relatively coarse mesh in the phonon wave vector space and the absolute vibrational enthalpies may not be fully converged, we are concerned only with differences in energies between competing structures within the same supercell and any systematic sampling errors should cancel out in these differences. With the inclusion of the zero-point vibrational energies, the $T=0$ K energies of {110} ({111}) oriented structures increase to 16.3(78.6)meV/H_2 above the {100} oriented structure.

The lowest enthalpy, $T=0$ K structure of $SiH_4(H_2)_2$ at $P=5.6$ GPa ($V=265.4$ Å^3) is pictured in Fig. 1. Shown is the conventional cell with four formula units while the unit cell given in Table I contains two formula units. SiH_4 groups are located on fcc sites with hydrogen atoms occupying positions at the tetrahedral vertices in the $[\bar{1}\bar{1}\bar{1}]$, $[11\bar{1}]$, $[1\bar{1}1]$, and $[\bar{1}11]$ directions at a distance of 1.480 Å from the central silicon atom. H_2 are found in all of the octahedral and half the tetrahedral voids and are oriented in the [100] direction; the occupied tetrahedral positions correspond to those that are filled in the diamond cubic crystal structure.

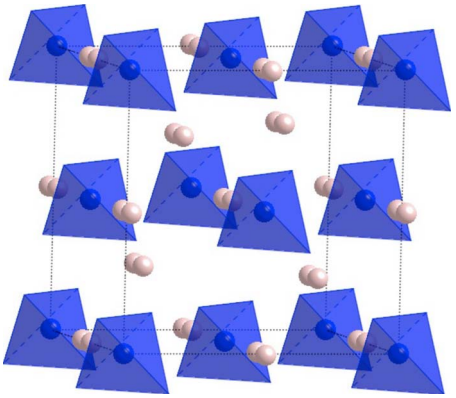

FIG. 1. (Color online) Proposed conventional cell of $SiH_4(H_2)_2$. Pink (light) spheres represent hydrogen atoms in H_2. Blue (dark) spheres represent silicon atoms and the surrounding tetrahedra show the orientation of the SiH_4 groups where hydrogen atoms are positioned at the vertices.

In order to understand the SiH_4-H_2 interaction and weakening of the H_2 bond in $SiH_4(H_2)_2$ under applied pressure, we have calculated the H_2 vibrational frequencies, electronic density of states (EDOS), and distances between various hydrogen atoms using the $T=0$ K structure in Fig. 1. The results for the intramolecular H_2 modes given in Fig. 2(a) and are in good agreement with the experimental Raman data; these show a decrease in the vibrational frequencies of H_2 in $SiH_4(H_2)_2$ with increasing pressure,[2] contrary to the behavior of bulk H_2 in which these frequencies increase.[5] Two distinct frequencies are seen at each pressure corresponding to the octahedral H_2 and tetrahedral H_2 peaks. A general decrease in the frequencies with increasing pressure is seen for H_2 at both sites (apart from a slight increase in the frequencies of octahedral H_2 up to 12.5 GPa), showing that the H_2 bond is weakening at each site. However, this decrease is much more rapid for tetrahedral H_2 than for octahedral H_2, suggesting that the bond softening effect is much larger for the former.

Experimental Raman spectra clearly show the presence of multiple peaks within a frequency interval of 100 cm^{-1} centered around 4175 cm^{-1}.[2] While the data in Fig. 2(a) confirm substantial frequency differences between the two types of H_2 molecules, it does not address the existence of interme-

TABLE I. Unit cell for the proposed structure of $SiH_4(H_2)_2$ with the conventional cell lattice parameter set to $a=6.426$ Å.

Space group		$I\bar{4}m2$		
Lattice parameters (Å)	a	4.601	α	90°
	b	4.601	β	90°
	c	6.268	γ	90°
		x	y	z
Wyckoff sites	Si	0.000	0.000	0.000
	H_1	0.500	0.237	0.364
	H_2	0.000	0.000	0.560
	H_3	0.000	0.500	0.310

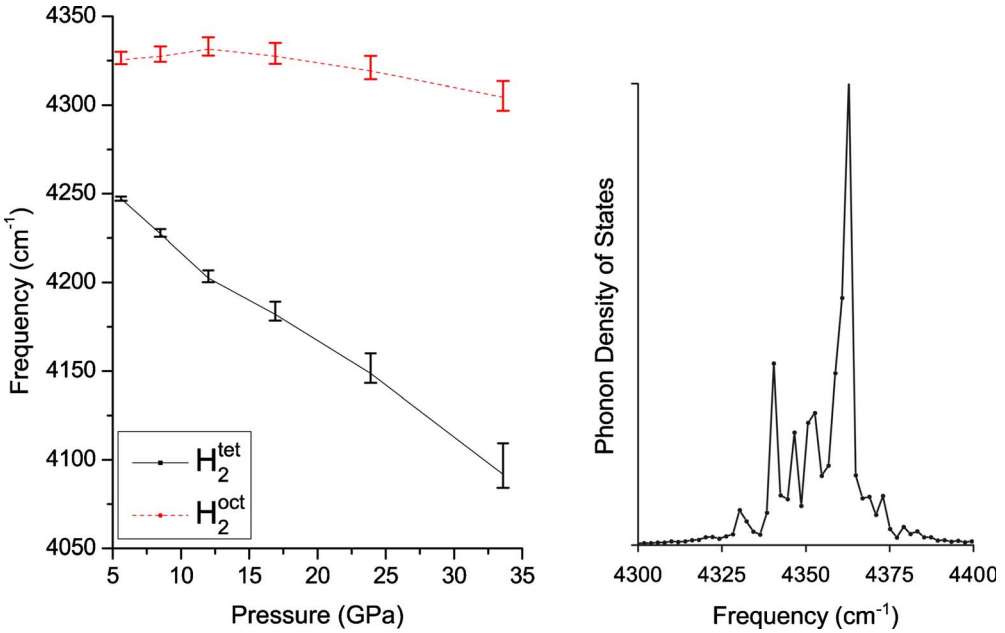

FIG. 2. (Color online) (a) Calculated H_2 vibrational frequencies in the $T=0$ K structure of $SiH_4(H_2)_2$ as a function of pressure. Points on the continuous lines give the average frequencies of H_2 in their respective sites. Bars show the range of frequencies for the two sites. (b) Phonon density of states for H_2 in $SiH_4(H_2)_2$ at $T=300$ K.

diate frequency vibrations. To demonstrate that these vibrations arise from thermal disordering of the H_2 orientations, we have performed *ab initio* molecular dynamics calculations of the temperature-dependent phonon density of states (PDOS) at $P=5.6$ GPa [see Fig. 2(b)]. The PDOS is obtained by taking the Fourier transform of the mass-weighted velocity autocorrelation function[14] such that

$$g(\mathbf{k},\omega) = \int e^{i\omega t} dt \sum_n e^{-i\mathbf{k}\cdot\mathbf{R}_n} \frac{\langle \mathbf{v}_n(t)\cdot\mathbf{v}_0(0)\rangle}{\langle \mathbf{v}_n(0)\cdot\mathbf{v}_0(0)\rangle}, \qquad (1)$$

where $\mathbf{R}_n$ and $\mathbf{v}_n$ are the lattice position and velocity of the nth hydrogen atom, $\mathbf{k}$ is the wave vector, and ω is the frequency. The positions and velocities are taken from *ab initio* molecular dynamics simulations in VASP over 40 ps with time steps of 0.5 fs, giving a frequency resolution of 2 cm^{-1}. The temperature is controlled using the Nose-Hoover thermostat[15,16] set to $T=300$ K. Figure 2 shows that while the PDOS for the $T=0$ K structure has only two distinct peaks, the temperature-dependent PDOS becomes more diffuse with a spread of 60 cm^{-1} and a greater number of peaks.

We observe rapid rotations and librations of H_2 molecules during our AIMD simulations, suggesting that thermal disorder at $P=5.6$ GPa destroys the static H_2 orientational ordering shown in Fig. 1. Broadening of the PDOS and appearance of additional spectral lines in Fig. 2 are both attributed to the interactions between H_2 vibrons and rotations. Although the width of the phonon distribution agrees well with experimental results, the positions of the peaks are calculated to be about 200 cm^{-1} higher than the measured frequencies. To address the importance of quantum effects, we have investigated the orientational dynamics of H_2 molecules using climbing image nudged elastic band calculations. We find rotational barriers of 11 meV for octahedral H_2 and 15 meV for tetrahedral H_2 and conclude that at room temperature, thermal excitations should result in significant rotation of both types. This conclusion agrees well with our AIMD trajectories. Since the rotational barriers are smaller than thermal energies, the treatment of this system using classic molecular dynamics is likely sufficient at 300 K but quantum effects such as tunneling and quadrupolar interactions between angular momentum quantum states could become important at lower temperatures. Unfortunately, quantum simulations of such phenomena are prohibitively expensive using DFT energetics and are beyond the scope of this study.

It is interesting to compare our results for $SiH_4(H_2)_2$ with the behavior of solid H_2. As a function of temperature and pressure, solid hydrogen exists in one of the three phases commonly represented by I, II, and III.[17,18] Phase I, where H_2 molecules occupy either the $J=0$ or 1 rotational quantum states and align by their angular momenta, exists at low pressures and/or high temperatures. Phase II exists at low temperatures and low pressures (up to approximately 150 GPa) where H_2 occupy higher J states and again align by their angular momenta. Finally, at higher pressures, phase III exists in which interactions between H_2 molecules become so strong that the molecules order classically. The H_2 Raman-active vibrons (corresponding to in-phase H_2 vibrations) show rapid softening above $P=40$ GPa while the frequencies of infrared-active vibron frequencies (corresponding to out-of-phase H_2 vibrations) increase until 120 GPa and start decreasing at higher pressures. By comparing this behavior with the data presented in Fig. 2, it can be hypothesized that H_2 molecules in $SiH_4(H_2)_2$ experience local pressures resembling the conditions at the boundary of Phases II and III of

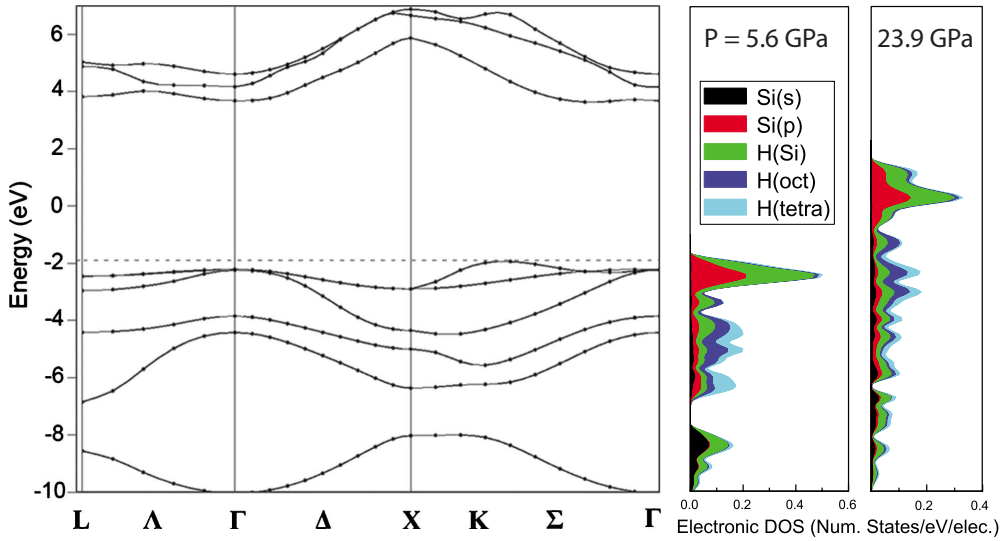

FIG. 3. (Color online) Calculated electronic band structure of $SiH_4(H_2)_2$ at a pressure of 5.6 GPa (with Γ to X being perpendicular to H_2 orientations) and the electronic density of states at pressures of 5.6 and 23.9 GPa (Ref. 19).

solid H_2. Our $T=0$ K DFT calculations implicitly assume that H_2 molecules order in a manner similar to that of Phase III but it is possible that an ordered quantum solid may be stable at low pressures, behaving in a manner similar to Phase II of solid H_2. Furthermore, it remains an interesting open question whether orientational ordering of H_2 rotons, such as observed in Phase I of solid H_2, also exists in $SiH_4(H_2)_2$ at high temperatures.

The results of our EDOS calculations at pressures of 5.6 and 23.9 GPa are given in Fig. 3. The EDOS is shown for the Si(s) and Si(p) orbitals and for hydrogen in SiH_4 units, as well as for H_2 in octahedral and tetrahedral sites. The average energies and band widths [given by $W^2=\int(E-E_0)^2g(E)dE$, where $E_0=\int E\cdot g(E)dE$ is the position of the band center] are calculated for all orbitals at each pressure. At the lower pressure, the band widths for octahedral and tetrahedral H_2 are 1.43 eV and 1.70 eV, respectively; these values increase to 2.29 and 2.62 eV at the higher pressure. At each of these pressures, the band width is larger for tetrahedral H_2 than octahedral H_2, showing a higher degree of hybridization with SiH_4 units for the former. As the pressure is increased, the band width increases for both H_2 types suggesting that their orbitals further hybridize with SiH_4, subsequently weakening the H_2 bonds and lowering their intramolecular vibrational frequencies. Furthermore, the band gap of 5.8 eV at $P=5.6$ GPa has a calculated reduction to 3.7 eV at $P=23.9$ GPa, which is in-line with experimental results that suggest a reduction in the band gap with increasing pressure.[2]

The effect of pressure on the H-H and Si-H bond lengths is given in Table II. These results show that there is an increase in the bond length of H_2 located at tetrahedral sites with pressure. This corresponds to a weakening of the H_2 bond, following results of both phonon mode and electronic DOS calculations. However, the bond length of H_2 located in octahedral sites slightly decreases with increasing pressure; this suggests that the bond is becoming stronger, seemingly opposing previous results. This contradiction may be attributed to steric effects where the increasingly (with pressure) limited physical space available for octahedral H_2 results in a reduction in its bond length. Finally, the values of $d(H_2\text{-}SiH_4)^{near}$ (smaller for H_2 in octahedral than tetrahedral

TABLE II. Lengths of both H-H and Si-H bonds are given as a function of pressure. The nearest distances from hydrogen atoms in SiH_4 units to hydrogen in H_2 are also given. Finally, the average distances between hydrogen in H_2 and all hydrogen atoms in nearest-neighbor SiH_4 (four nearest-neighbor groups for tetrahedral H_2 and six for octahedral) are shown in the final two columns. All lengths are given in angstrom, volume in cubic angstrom, and pressure in gigapascal.

Vol. (c.c.)	Pressure	H-H bond length		Si-H bond length	$d(H_2\text{-}SiH_4)^{near}$		$d(H_2\text{-}SiH_4)^{avg}$	
		Octahedral	Tetrahedral		Octahedral	Tetrahedral	Octahedral	Tetrahedral
265.4	5.6	0.748	0.752	1.480	2.257	2.318	3.283	2.906
241.2	8.5	0.747	0.753	1.475	2.196	2.240	3.188	2.826
221.4	12.0	0.747	0.754	1.470	2.129	2.178	3.105	2.758
202.8	16.9	0.746	0.754	1.463	2.060	2.106	3.023	2.690
185.2	23.9	0.746	0.756	1.453	1.993	2.041	2.999	2.621
168.7	33.6	0.746	0.758	1.440	1.924	1.971	2.855	2.550

sites) seem to suggest that there should be a greater hybridization of SiH_4 with octahedral H_2 than with tetrahedral H_2; however, this is contradicted by the results of electronic DOS calculations. This perceived discrepancy may be explained by average distances between hydrogen in H_2 and hydrogen in SiH_4, $d(H_2\text{-}SiH_4)^{avg}$ in Table II, rather than by nearest neighbors. These results show that $d(H_2\text{-}SiH_4)^{avg}$ is smaller for tetrahedral H_2 than for octahedral H_2, accounting for the greater degree of hybridization between SiH_4 and H_2 in tetrahedral sites.

IV. CONCLUSIONS

In summary, a structure for $SiH_4(H_2)_2$ under an applied pressure of 5.6 GPa has been proposed that belongs to the $I\bar{4}m2$ space group. In the conventional cell, SiH_4 groups are found at fcc sites with H_2 in each of the octahedral sites and in one half of the tetrahedral sites, occupied in a diamondlike fashion. SiH_4 units are oriented such that hydrogen atoms are pointing toward the unoccupied tetrahedral sites. H_2 molecules are oriented along the [100] direction in the $T=0$ K structure but it is found that orientational disorder occurs at room temperature. A weakening of the H_2 bond with increasing pressure is seen in the corresponding decrease in H_2 phonon-mode frequencies. This behavior is attributed to a greater degree of hybridization of H_2 and SiH_4 orbitals as the pressure is increased.

ACKNOWLEDGMENTS

This work was supported by the U.S. Department of Energy, Office of Science, Basic Energy Sciences under Grant No. DE-FG02–05ER46253. Resources were used from the National Energy Research Scientific Computing Center (NERSC).

*vidvuds@ucla.edu

[1] S. ichi Orimo, Y. Nakamori, J. R. Eliseo, A. Zuettel, and C. M. Jensen, Chem. Rev. **107**, 4111 (2007).
[2] T. A. Strobel, M. Somayazulu, and R. J. Hemley, Phys. Rev. Lett. **103**, 065701 (2009).
[3] N. W. Ashcroft, Phys. **2**, 65 (2009).
[4] S. Satyapal, J. Petrovic, C. Read, G. Thomas, and G. Ordaz, Catal. Today **120**, 246 (2007).
[5] P. Loubeyre, R. Letoullec, and J. P. Pinceaux, Phys. Rev. Lett. **72**, 1360 (1994).
[6] B. Magyari-Köpe, V. Ozolins, and C. Wolverton, Phys. Rev. B **73**, 220101(R) (2006).
[7] G. Kresse and J. Furthmuller, Phys. Rev. B **54**, 11169 (1996).
[8] P. E. Blöchl, Phys. Rev. B **50**, 17953 (1994).
[9] J. P. Perdew and Y. Wang, Phys. Rev. B **45**, 13244 (1992).
[10] H. J. Monkhorst and J. D. Pack, Phys. Rev. B **13**, 5188 (1976).
[11] H. Jónsson, G. Mills, and K. W. Jacobsen, *Classical and Quantum Dynamics in Condensed Phase Simulations* (World Scientific, Singapore, 1998).
[12] The quoted values include only the internal energy calculated at constant volume. Adjusting the volume of each configuration to achieve constant pressure would affect the relative enthalpies by $\Delta H=(V/2B)\Delta P^2$ where B is the bulk modulus and ΔP is the deviation from the target pressure. Since the calculated values of ΔP are less than 1 kbar, these corrections are less than 0.1 meV/H_2.
[13] C. Wolverton, V. Ozolins, and M. Asta, Phys. Rev. B **69**, 144109 (2004).
[14] C. Z. Wang, C. T. Chan, and K. M. Ho, Phys. Rev. B **42**, 11276 (1990).
[15] S. Nosé, J. Chem. Phys. **81**, 511 (1984).
[16] W. G. Hoover, Phys. Rev. A **31**, 1695 (1985).
[17] I. I. Mazin, R. J. Hemley, A. F. Goncharov, M. Hanfland, and H.-k. Mao, Phys. Rev. Lett. **78**, 1066 (1997).
[18] I. F. Silvera, S. J. Jeon, and H. E. Lorenzana, Phys. Rev. B **46**, 5791 (1992).
[19] The electronic structure of $SiH_4(H_2)_2$ was obtained with QUANTUM ESPRESSO (Ref. 20) using norm-conserving pseudopotentials, a plane-wave cutoff energy of 50 Ry and $4\times4\times4$ **k**-point mesh.
[20] P. Giannozzi, S. Baroni, N. Bonini, M. Calandra, R. Car, C. Cavazzoni, D. Ceresoli, G. L. Chiarotti, M. Cococcioni, I. Dabo, A. D. Corso, S. d. Gironcoli, S. Fabris, G. Fratesi, R. Gebauer, U. Gerstmann, C. Gougoussis, A. Kokalj, M. Lazzeri, L. Martin-Samos, N. Marzari, F. Mauri, R. Mazzarello, S. Paolini, A. Pasquarello, L. Paulatto, C. Sbraccia, S. Scandolo, G. Sclauzero, A. P. Seitsonen, A. Smogunov, P. Umari, and R. M. Wentzcovitch, J. Phys.: Condens. Matter **21**, 395502 (2009).